BIOLOGY, MEDICINE, & NATURAL PRODUCT CHEMISTRY ISSN 2089-6514 (paper)
Volume 15, Number 1, April 2026 | Pages: 861-880 | DOI: 10.14421/biomedich.2026.151.861-880 ISSN 2540-9328 (online)

Virulence Factors of Gastrointestinal Pathogens *Escherichia coli*, *Salmonella enterica*, and *Proteus mirabilis* Targeted by Luteolin: A Microbioinformatics Study

Muhammad Sulthan Rizqy Syamsuddin[1], Rian Ka Praja[2,*], Nawan[2], Astrid Teresa[3], Agnes Frethernety[4]
[1]Faculty of Medicine; [2]Department of Microbiology, Faculty of Medicine;
[3]Departement of Clinical Medicine, Faculty of Medicine; [4]Departement of Pharmacotherapy, Faculty of Medicine,
Universitas Palangka Raya
Jl. H. Timang, Palangka Raya, Indonesia.

Corresponding author*
riankapraja@med.upr.ac.id

Manuscript received: 23 December 2025. Revision accepted: 13 April 2026, Published: 11 June 2026.

Abstract

Luteolin is a natural flavonoid with broad-spectrum antibacterial, anti-inflammatory, and metabolic regulatory properties, making it a promising antivirulence candidate against gastrointestinal pathogens such as *Escherichia coli* ATCC8739, *Salmonella enterica* CT18, and *Proteus mirabilis* HI4320. The increasing global burden of antimicrobial resistance highlights the need for alternative strategies targeting virulence rather than bacterial viability. This study aimed to investigate the interaction of luteolin with virulence-associated proteins of these pathogens using a microbioinformatics-based approach. Protein–compound interaction networks were analyzed using STITCH v5.0, and the resulting FASTA sequences were evaluated using VICMPred, VirulentPred, BepiPred v1.0, MHC I and II Binding Predictions, and PSORTb v3.0 to determine functional classes, virulence potential, immunogenic epitopes, and subcellular localization. The analysis identified multiple virulent proteins targeted by luteolin in each pathogen: cirA, ECs4935, yedX, rbbA, pykA, and pykF in *E. coli*; fepA, iroN, iroB, sitA, and pykF in *S. enterica*; and ireA and PMI2409 in *P. mirabilis*. These proteins are associated with outer membrane iron acquisition, epithelial adhesion, energy metabolism, and cellular homeostasis. Epitope prediction revealed numerous high-scoring B-cell and T-cell binding regions across all virulent proteins, indicating strong immunogenic potential, while subcellular localization analysis showed dominant outer membrane positioning for siderophore receptors and cytoplasmic localization for metabolic enzymes. The collective findings demonstrate that luteolin may exert antivirulence effects by interfering with iron uptake systems, destabilizing membrane-associated processes, and disrupting metabolic pathways essential for colonization and persistence, supporting its potential as a complementary therapeutic agent against enteric bacterial infections.

Keywords: *Escherichia coli;* Virulence Factor; Luteolin; *Salmonella enterica*; *Proteus mirabilis*

Abbreviations: ATP = Adenosine Triphosphate; BepiPred = B-epitope Prediction; DNA = Deoxyribonucleic Acid; FASTA = Fast Adaptive Shrinkage Threshold Algorithm; MHC = Major Histocompatibility Complex; MIC = Minimum Inhibitory Concentration; NCBI = National Center for Biotechnology Information; PSORTb = Prediction of Bacterial Protein Subcellular Localization; STITCH = Search Tool for Interacting Chemicals; SVM = Support Vector Machine; VICMPred = Virulence Factors Identification and Classification Using Machine Learning Prediction.

INTRODUCTION

Gastrointestinal infectious diseases continue to be a major public health burden globally, particularly in regions with limited sanitation and healthcare access (Murray et al., 2022). These infections frequently involve Gram-negative enteric pathogens such as *Escherichia coli*, *Salmonella enterica*, and *Proteus mirabilis*, which are responsible for diarrheal illness, enteric fever, urinary tract infections, and systemic complications (Jajere, 2019; Campos et al., 2019; Chakkour et al., 2024). The pathogenicity of these bacteria is largely determined by their virulence factors, including adhesion, biofilm formation, toxin production, iron acquisition, and metabolic adaptation, enabling efficient colonization and persistence in the host (Naidoo & Zishiri, 2025; Pakbin et al., 2021). Antimicrobial resistance (AMR) among these pathogens has escalated significantly, driven by misuse and overuse of antibiotics in human and agricultural settings (Kemenkes RI, 2021; Putri et al., 2023). This growing threat underscores the need for alternative therapeutic strategies that target bacterial virulence mechanisms without relying solely on conventional antibiotics.

Luteolin, a flavonoid commonly found in celery, broccoli, and other medicinal plants, has gained attention

as a natural compound with broad biological activities, including antibacterial, anti-inflammatory, and antioxidant properties (Salehi et al., 2019; Chagas et al., 2022). Several studies have reported that luteolin can inhibit key bacterial survival pathways, such as DNA gyrase activity in *E. coli*, membrane integrity, efflux pump function, metabolic energy production, and oxidative stress response (Liu et al., 2024; Gu & Pang, 2025). In *S. enterica*, luteolin reduces epithelial inflammation and reactive oxygen species without directly affecting bacterial adhesion, suggesting a modulatory rather than bactericidal mechanism (Tráj et al., 2023). Although direct evidence of luteolin's action on *P. mirabilis* is limited, related studies indicate its potential to disrupt quorum sensing, inhibit biofilm formation, and enhance antibiotic effectiveness in Gram-negative bacteria (Kovács et al., 2024). These findings support luteolin's promise as an antivirulence agent capable of weakening pathogenic processes while reducing selective pressure for resistance.

Recent advancements in microbioinformatics allow rapid, high-resolution prediction of compound–protein interactions, virulence profiles, immunogenic epitopes, and subcellular localization. Tools such as STITCH, VICMPred, VirulentPred, BepiPred, and MHC BindingPred enable computational exploration of bacterial proteins and their functional relevance in pathogenicity (Szklarczyk et al., 2016; Kashyap et al., 2020; Sharma et al., 2023). These tools have been widely used to identify potential biosignatures for drug targeting and vaccine design, offering a cost-effective alternative to early-stage laboratory experiments (Amanda et al., 2025). Applying this integrated computational framework to luteolin and key gastrointestinal pathogens offers an opportunity to identify molecular targets involved in iron acquisition, membrane-associated processes, and metabolic regulation.

Based on these considerations, the present study investigates the interaction of luteolin with virulence-associated proteins of *E. coli* ATCC8739, *S. enterica* CT18, and *P. mirabilis* HI4320 using a comprehensive microbioinformatics approach. The analysis includes functional classification, virulence prediction, B-cell and T-cell epitope mapping, and subcellular localization profiling. The results are expected to provide deeper insights into luteolin's antivirulence potential and highlight protein targets that may serve as foundations for the development of future antibacterial therapies.

MATERIALS AND METHODS

Study area

This study used bioinformatics computational methods to analyze the bioactivity of *Escherichia coli*, *Salmonella enterica*, and *Proteus mirabilis* strains targeted by flavonoid components, namely luteolin. The *h*ardware material used in this study was a set of Asus VivoBook X415MA-PC1411CMA laptops with Intel Celeron processors, 4.0 GB RAM, and connected to the internet. The software used for data analysis was bioinformatics software, namely STITCH v5.0, VICMPred, VirulentPred, BepiPred v1.0, MHC BindPred, and PSORTb v3.0.

Inclusions and Exclusions Criteria

Inclusions

1. *Escherichia coli* ATCC8739, *Salmonella enterica* CT18, and *Proteus mirabilis* HI4320 proteins predicted to interact with luteolin based on the STITCH v5.0 interaction network.
2. FASTA sequences of *E. coli* ATCC8739, *S. enterica* CT18, and *P. mirabilis* HI4320 are available in the National Center for Biotechnology Information (NCBI) database.

Exclusions

1. The software being used cannot be accessed (such as network connection problems, internal server error, blocked IP, 404 not found).

Bacterial strain

The bacterial material used in this study consisted of FASTA sequences of *Escherichia coli* ATCC8739, *Salmonella enterica* CT18, and *Proteus mirabilis* HI4320 obtained from the National Center for Biotechnology Information (NCBI). *E. coli* ATCC8739 is a non-pathogenic reference strain frequently used in molecular studies and antimicrobial research (Naidoo & Zishiri, 2025). *S. enterica* CT18 represents a clinically important strain associated with enteric infections and has been widely used as a genomic reference in pathogenesis studies (Jajere, 2019). *P. mirabilis* HI4320 is a well-characterized uropathogenic strain known for its capacity to form biofilms, swarm on solid surfaces, and express iron-regulated outer membrane proteins essential for host colonization (Chakkour et al., 2024).

Procedures

1. Identify the interactions of *Escherichia coli* ATCC8739, *Salmonella enterica* CT18, and *Proteus mirabilis* HI4320 targeted by luteolin using the STITCH v5.0 platform, then download the corresponding FASTA sequences from the National Center for Biotechnology Information (NCBI).
2. Annotate the FASTA files according to the protein name and save them in different folders based on protein type and bacterial species
3. Use the FASTA files to identify the functional class, virulence properties, epitope characteristics, and subcellular localization of proteins from *E. coli* ATCC8739, *S. enterica* CT18, and *P. mirabilis* HI4320 that interact with luteolin using VICMPred, VirulentPred, BepiPred v1.0, MHC BindingPred, and PSORTb v3.0.

Data analysis

Protein interaction analysis

Analysis of the interaction between luteolin and proteins from *E. coli* ATCC8739, *S. enterica* CT18, and *P. mirabilis* HI4320 was performed using the Search Tool for Interacting Chemicals (STITCH), which integrates experimental, computational, and text-mined evidence to generate compound–protein interaction networks. STITCH is accessible at http://stitch.embl.de/. Enter the compound name "luteolin" and select the target bacterial species. The server displays a network map showing predicted interaction strength between luteolin and bacterial proteins. FASTA sequences of the interacting proteins were subsequently retrieved from NCBI for downstream computational analysis (Szklarczyk et al., 2016)

Analysis and interpretation of the functional class

Functional class prediction was conducted using VICMPred by uploading the FASTA sequences obtained earlier. VICMPred classifies proteins into one of four categories—virulence factors, information molecules, cellular processes, or metabolic molecules—based on the amino acid composition and SVM-based computational modeling (Kashyap et al., 2020). The data were submitted through the "SUBMISSION" page at https://webs.iitd.edu.in/, and results were recorded accordingly.

Virulence analysis

Virulence assessment of proteins from *Escherichia coli* ATCC8739, *Salmonella enterica* CT18, *and Proteus mirabilis* HI4320, which were targeted by luteolin, was performed using VirulentPred software. Previously obtained FASTA data were uploaded via the "Submit" page and then processed by pressing the "Submit sequence" button. This software uses a machine learning model trained with experimental data on proteins that will produce virulent and non-virulent proteins, and provides a prediction score based on these results (Sharma et al, 2020). Proteins identified as virulent were then further analyzed to determine their epitopes and subcellular locations. VirulentPred can be accessed through the website http://bioinfo.icgeb.re.in/virulent/.

Epitope B-cell analysis

B-cell epitope analysis on *Escherichia coli* ATCC8739, *Salmonella enterica* CT18, and *Proteus mirabilis* HI4320 proteins targeted by luteolin was performed using BepiPred v1.0 software. This process was carried out by uploading the FASTA format of the previously analyzed virulent proteins to the main page of the site, then pressing the "Submit" button. This software is used to predict linear B-cell epitopes in protein sequences using data from the antibody protein complex structure of potential epitopes and non-epitopes (Jespersen et al, 2017). Amino acids with a default threshold value of 0.350 were predicted as epitopes and are displayed in yellow on the graph. BepiPred v1.0 can be accessed through the site http://tools.iedb.org/bcell/.

T cell cytotoxic and helper T cell Epitope analysis

MHC I epitope analysis on *Escherichia coli* ATCC8739, *Salmonella enterica* CT18, and *Proteus mirabilis* HI4320 proteins targeted by luteolin was performed using the MHC I Binding Predictions feature available at http://tools.iedb.org/mhci/. MHC I BindingPred predicts short peptides, generally 9 amino acids long (9-mer), that bind to MHC class I molecules and are presented to cytotoxic T cells ($CD8^+$) (Jensen KK et al, 2018). The initial step is to enter the FASTA sequence of the protein that has been identified as virulent through previous analysis on the main page, either by typing it directly in the "Specify Sequence(s)" column or uploading it via the "Choose File" option. Select the "IEDB recommended 2023.05 (NetMHCIIpan 4.1 EL)" method. In the "Select species/locus" section, select "Human, HLA-DR," then specify the allele "HLA-A*11:01" and the peptide length "9." In the "Output" section, select the "Percentile Rank" option and click "Submit." The site will then display the epitope prediction results in the form of percentile rank values.

Sub-cellular localization analysis

Analysis of the subcellular location of proteins from *Escherichia coli* ATCC8739, *Salmonella enterica* CT18, and *Proteus mirabilis* HI4320, which were targeted by luteolin, was performed using PSORTb v3.0 software. The initial step was to select the organism type from the "Choose an organism type" menu on the main page, then select the Gram-positive option in the "Choose Gram stain" section. After that, protein data in FASTA format that had previously been identified as virulent were entered. PSORTb then analyzed the subcellular location of proteins in prokaryotic organisms. Protein locations such as the outer membrane, cytoplasm, periplasm, or cell wall (El-Rami et al, 2019). The analysis results are presented in tabular form tailored to the research objectives. PSORTb can be accessed through the website https://www.psort.org/psortb/.

RESULTS AND DISCUSSION

Result of Protein Interaction

a. Interaction of *Escherichia coli* ATCC8739 with Luteolin

Based on the interaction between luteolin and *Escherichia coli* ATCC8739, ten interacting proteins were identified: ECs4935, yahD, fepA, cirA, yedX, rbbA, pykA, pykF, htpG, and nudH. Of these ten proteins, it is known that several proteins interacting with luteolin also interact with each other, namely fepA and cirA

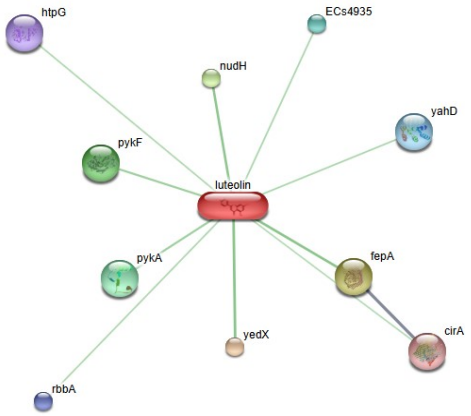

Figure 1. Results of Analysis of Luteolin Interaction with *Escherichia coli* ATCC8739

b. Interaction of *Salmonella enterica* CT18 with Luteolin

Based on the interaction between luteolin and *Salmonella enterica* CT18, ten proteins were found to interact, namely STY4224, pykF, hiuH, pykA, htpG, fepA, sitA, iroN, iroB, and rppH. Of the ten proteins, it is known that several proteins that interact with luteolin also interact with each other, namely fepA, sitA, iroN, and iroB.

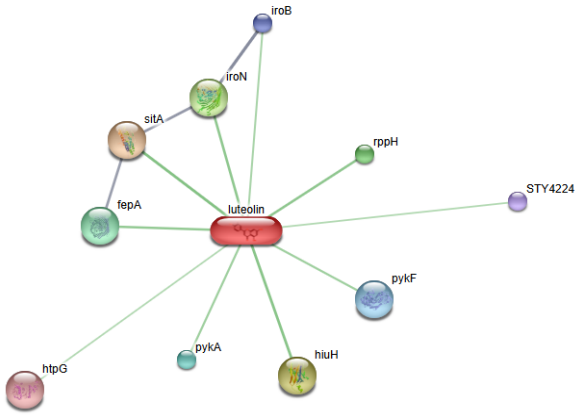

Figure 2. Results of Analysis of Luteolin Interaction with *Salmonella enterica* CT18

c. Interaction of *Proteus mirabilis* HI4320 with Luteolin

Based on the interaction between luteolin and *Proteus mirabilis* HI4320, ten proteins were found to interact, namely PMI2409, htpG, rppH, PMI1224, pykA, pykF, PMI0842, cysj, ireA, sitA. Of the ten proteins, it is known that several proteins that interact with luteolin also interact with each other, namely sitA and ireA.

Figure 3. Results of Analysis of Luteolin Interaction with *Proteus mirabilis* HI4320

Functional class and virulence analysis is a further step in protein interaction analysis. *Escherichia coli* ATCC8739, *Salmonella enterica* CT18, and *Proteus mirabilis* HI4320 interacting with luteolin were analyzed using two tools at this stage: VICMPred at https://webs.iiitd.edu.in/raghava/vicmpred/submission.html and VirulentPred at http://bioinfo.icgeb.res.in/virulent/.

Table 1. Analysis Results of Functional Classes and Virulence Properties of *Escherichia coli* ATCC8739 Proteins Interacting with Luteolin.

Organism	Identifier	Proteins that interact with luteolin	Functional class	Virulent properties	Virulence score
Escherichia coli ATCC8739	ECs4935	ShET2 enterotoxin domain-containing protein	Cellular process	Virulent	0.9992
	yahD	K06867	Metabolism Molecule	Non-Virulent	-0.856
	fepA	outer membrane receptor FepA	Cellular process	Non-Virulent	-0.125
	cirA	colicin I receptor	Cellular process	Virulent	1.1032
	yedX	hydroxyisourate hydrolase	Cellular process	Virulent	0.4768
	rbbA	ABC transporter-like protein	Metabolism Molecule	Virulent	1.0460
	pykA	pyruvate kinase	Virulence factors	Virulent	0.0256
	pykF	pyruvate kinase	Metabolism Molecule	Virulent	0.1618

Organism	Identifier	Proteins that interact with luteolin	Functional class	Virulent properties	Virulence score
	htpG	heat shock protein 90; Molecular chaperone. Has ATPase activity	Cellular process	Non-Virulent	-1.000
	nudH	dinucleoside polyphosphate hydrolase; Accelerates the degradation of transcripts by removing pyrophosphate from the 5'-end of triphosphorylated RNA, leading to a more labile monophosphorylated state that can stimulate subsequent ribonuclease cleavage	Cellular process	Non-Virulent	-0.815

The results of the functional class analysis and virulence properties of *Escherichia coli* ATCC8739 proteins interacting with luteolin showed three functional classes, namely cellular processes, virulence factors, and metabolism molecules. The analysis identified four proteins with non-virulent properties, namely yahD, fepA, htpG, and nudH, and six proteins with virulent properties, namely ECs4935, cirA, yedX, rbbA, pykA, and pykF, each having virulence scores of 0.9992, 1.1032, 0.4768, 1.0460, 0.0256, and 0.1618, respectively.

Table 2. Analysis Results of Functional Classes and Virulence Properties of *Salmonella enterica* CT18 Proteins Interacting with Luteolin.

Organism	Identifier	Proteins that interact with luteolin	Functional class	Virulent properties	Virulence score
Salmonella enterica CT18	STY4224	ABC transporter ATP-binding protein	Metabolism Molecule	Non-Virulent	-1.033
	pykF	pyruvate kinase	Metabolism Molecule	Virulent	0.8703
	hiuH	hypothetical protein; Catalyzes the hydrolysis of 5-hydroxyisourate (HIU) to 2-oxo-4-hydroxy-4-carboxy-5-ureidoimidazoline (OHCU)	Cellular process	Non-Virulent	-0.731
	pykA	pyruvate kinase	Virulence factors	Non-Virulent	-0.337
	htpG	heat shock protein 90; Molecular chaperone. Has ATPase activity	Virulence factors	Non-Virulent	-1.002
	fepA	outer membrane receptor FepA	Virulence factors	Virulent	0.9855
	sitA	Iron transport protein periplasmic-binding protein	Metabolism Molecule	Virulent	0.8061
	iroN	outer membrane receptor FepA	Virulence factors	Virulent	1.1056
	iroB	glycosyltransferase	Cellular process	Virulent	0.2088
	rppH	dinucleoside polyphosphate hydrolase; Accelerates the degradation of transcripts by removing pyrophosphate from the 5'-end of triphosphorylated RNA, leading to a more labile monophosphorylated state that can stimulate subsequent ribonuclease cleavage	Cellular process	Non-Virulent	-0.993

The results of the functional class analysis and virulence properties of *Salmonella enterica* CT18 proteins interacting with luteolin showed three functional classes, namely cellular processes, virulence factors, and metabolism molecules. The analysis identified five proteins with non-virulent properties, namely STY4224, hiuH, pykA, htpG, and rppH, and five proteins with virulent properties, namely pykF, fepA, sitA, iroN, and iroB, each having virulence scores of 0.8703, 0.9855, 0.8061, 1.1056, and 0. 0.2088, respectively.

Table 3. Analysis Results of Functional Classes and Virulence Properties of *Proteus mirabilis* HI4320 Proteins Interacting with Luteolin.

Organism	Identifier	Proteins that interact with luteolin	Functional class	Virulent properties	Virulence score
Proteus mirabilis HI4320	htpG	heat shock protein 90; Molecular chaperone. Has ATPase activity	Cellular process	Non-Virulent	-1.000
	rppH	dinucleoside polyphosphate hydrolase; Accelerates the degradation of transcripts by removing pyrophosphate from the 5'-	Metabolism Molecule	Non-Virulent	-1.106

Organism	Identifier	Proteins that interact with luteolin	Functional class	Virulent properties	Virulence score
		end of triphosphorylated RNA, leading to a more labile monophosphorylated state that can stimulate subsequent ribonuclease cleavage.			
	PMI1224	multidrug ABC transporter	Metabolism Molecule	Non-Virulent	-1.028
	pykA	pyruvate kinase	Metabolism Molecule	Non-Virulent	-0.519
	pykF	pyruvate kinase	Metabolism Molecule	Non-Virulent	-0.156
	PMI0842	outer membrane receptor	Virulence factors	Non-Virulent	-0.368
	cysJ	sulfite reductase [NADPH] flavoprotein alpha-component; Component of the sulfite reductase complex that catalyzes the 6-electron reduction of sulfite to sulfide. This is one of several activities required for the biosynthesis of L- cysteine from sulfate. The flavoprotein component catalyzes the electron flow from NADPH -> FAD -> FMN to the hemoprotein component	Virulence factors	Non-Virulent	-1.031
	sitA	iron ABC transporter substrate-binding protein	Virulence factors	Non-Virulent	-0.998
	ireA	iron-regulated outer membrane virulence protein	Virulence factors	Virulent	1.0045
	PMI2409	pyruvate kinase	Metabolism Molecule	Virulent	1.0365

The results of the functional class analysis and virulence properties of *Proteus mirabilis* HI4320 proteins interacting with luteolin showed three functional classes, namely cellular processes, virulence factors, and metabolic molecules. The analysis identified eight proteins with non-virulent properties, namely htpG, rppH, PMI1224, pykA, pykF, PMI0842, cysJ, and sitA, as well as two proteins with virulent properties, namely ireA, and PMI2409, each having a virulence score of 1.0045 and 1.0365, respectively.

B-cell Epitope Analysis

B-cell epitope analysis was performed as a follow-up step after obtaining the functional classification and identification of the virulence properties of *Escherichia coli* ATCC8739, *Salmonella enterica* CT18, and *Proteus mirabilis* HI4320 proteins interacting with luteolin. This analysis utilized BepiPred v1.0 from the website http://tools.iedb.org/bcell/ , focusing on proteins with virulent properties. The analysis resulted in amino acid sequences that bind to B cells (epitopes) and those that do not bind (non-epitopes).

These amino acid sequences were visualized in two color graphs, green and yellow, using a threshold value of 0.350. The green graph indicates amino acid sequences that do not bind to B cells (non-epitopes) with a value <0.350, while the yellow graph indicates sequences that bind to B cells (epitopes) with a value >0.350.

a. Escherichia coli ATCC8739

B-cell epitope analysis in *Escherichia coli* ATCC8739 that interacts with luteolin was performed on the virulent proteins ECs4935, cirA, yedX, rbbA, pykA, and pykF. The analysis results indicate the presence of several amino acid chain sequences that act as B-cell epitopes, which are shown in the yellow graph.

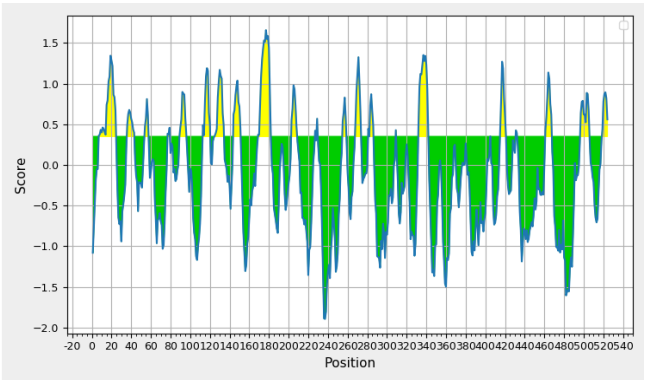

Figure 4. Results of Epitope Analysis of B-Cell ECs4935 Interacting with Luteolin

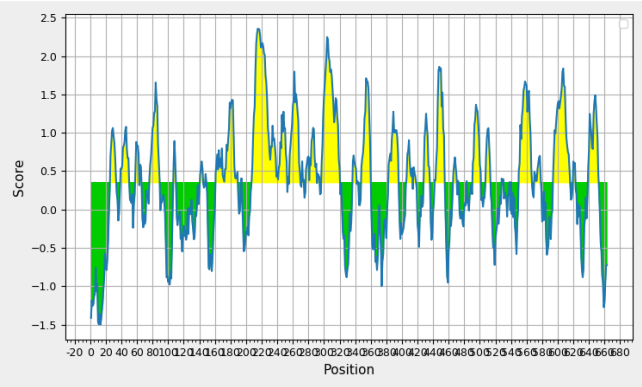

Figure 5. Results of Epitope Analysis of B-Cell cirA Interacting with Luteolin.

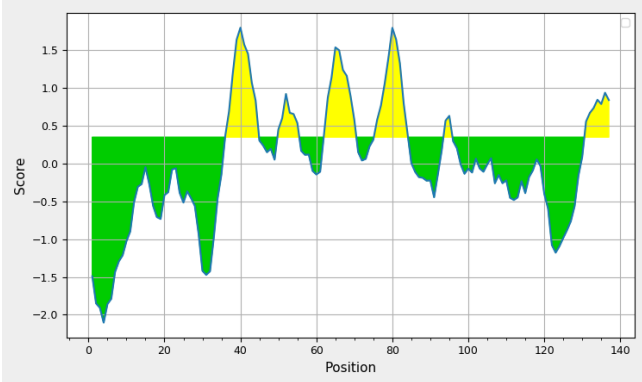

Figure 6. Results of Epitope Analysis of B-Cell yedX Interacting with Luteolin.

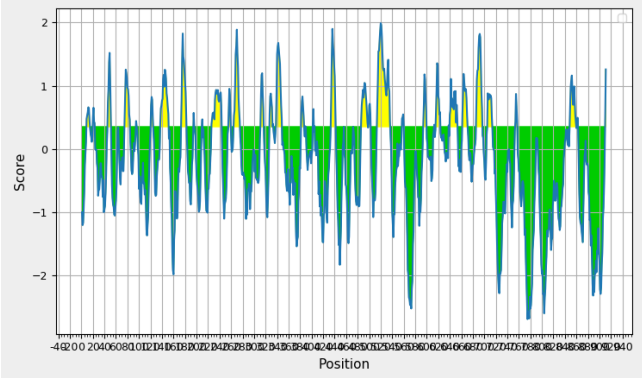

Figure 7. Results of Epitope Analysis of B-Cell **rbbA** Interacting with Luteolin.

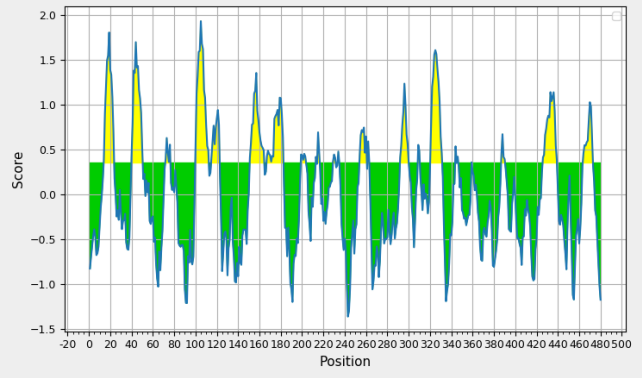

Figure 8. Results of Epitope Analysis of B-Cell pykA Interacting with Luteolin.

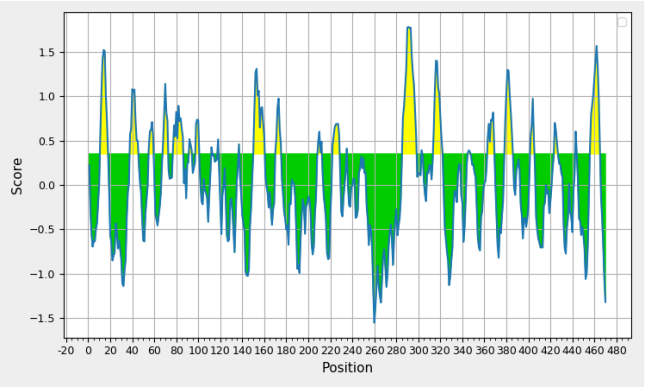

Figure 9. Results of Epitope Analysis of B-Cell pykF Interacting with Luteolin.

b. Salmonella enterica CT18

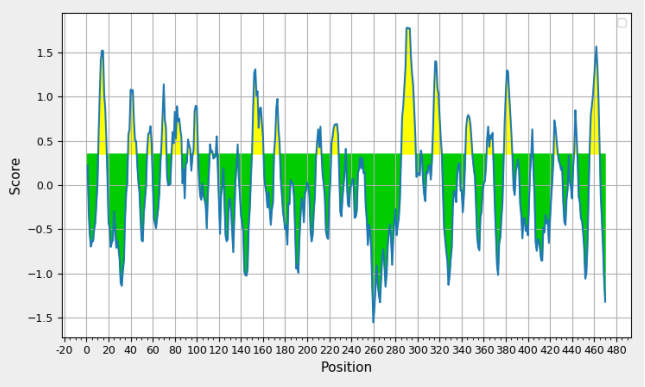

Figure 10. Results of Epitope Analysis of B-Cell pykF Interacting with Luteolin.

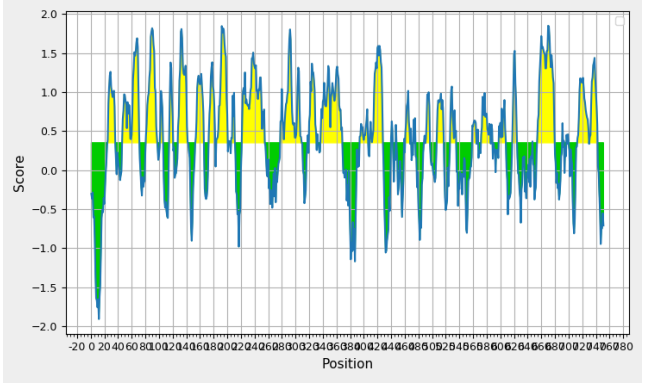

Figure 11. Results of Epitope Analysis of B-Cell fepA Interacting with Luteolin.

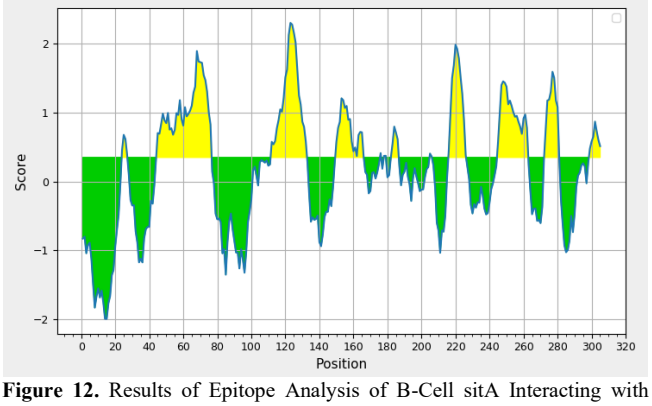

Figure 12. Results of Epitope Analysis of B-Cell sitA Interacting with Luteolin.

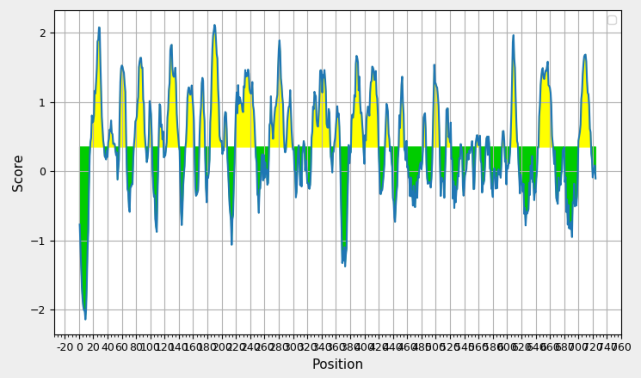

Figure 13. Results of Epitope Analysis of B-Cell iroN Interacting with Luteolin.

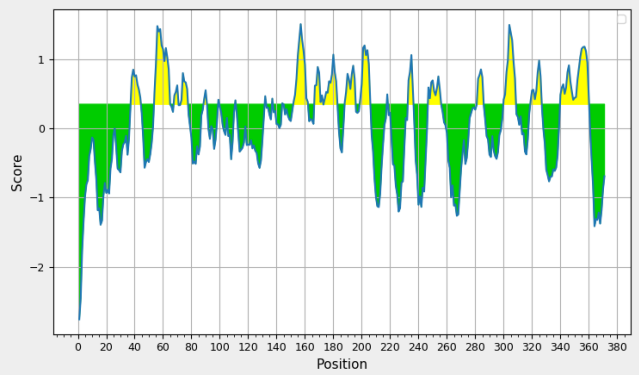

Figure 14. Results of Epitope Analysis of B-Cell iroB Interacting with Luteolin

c. *Proteus mirabilis* HI4320

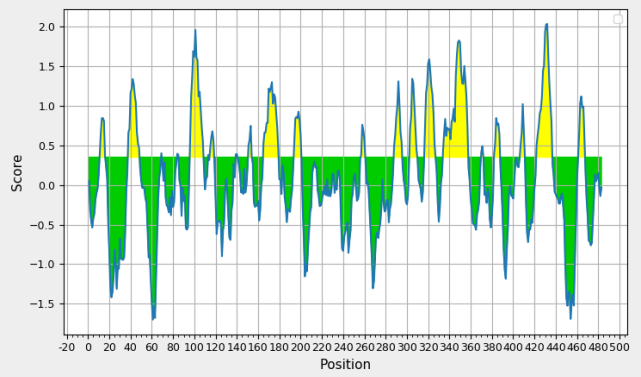

Figure 15. Results of Epitope Analysis of B-Cell PMI2409 Interacting with Luteolin.

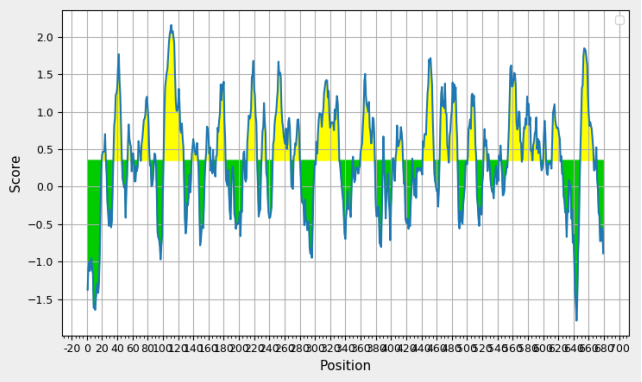

Figure 16. Results of Epitope Analysis of B-Cell ireA Interacting with Luteolin.

MHC I and MHC II Analysis Results

MHC I and MHC II analysis was conducted to identify *Escherichia coli* ATCC8739, *Salmonella enterica* CT18, and *Proteus mirabilis* HI4320 proteins that interact with luteolin as epitopes on T cells. This process uses MHC I Binding Predictions through the site http://tools.iedb.org/mhci/ and MHC II Binding Predictions through http://tools.iedb.org/mhcii/, involving virulent proteins as the object of study. The results of the analysis on each protein produce peptide chains that have the potential to bind to T cells (epitopes), accompanied by their values and rankings.

MHC I

MHC I analysis uses the HLA-A*11:01 allele, which is the most common allele in Asian populations. The average MHC I epitope has a peptide chain length of nine amino acids.

a. *Escherichia coli* ATCC 8749

The results of the MHC I analysis of *Escherichia coli* ATCC8739, the ECs4935 protein showed the highest score of 0.96 with the QTLSELFYK peptide chain, in the cirA protein the highest score was 0.94 with the GVVNIITK peptide chain, in the yedX protein the highest score was 0.68 with the SQYGYSTYR peptide chain, the rbbA protein obtained the highest score of 0.80 with the SALSVVREK peptide chain, in the pykA protein the highest score was 0.87 with the AMYAANHLK peptide chain, while in the pykF protein the highest score was 0.86 with the QTFTFTTDK peptide chain.

Table 4. MHC I ECs4935 Analysis Results.

No	*Allele*	*Start*	*End*	*Length*	*Peptide*	*Score*	*Percentile Rank*
1	HLA-A*11:01	24	32	9	QTLSELFYK	0.96	0.01
2	HLA-A*11:01	1	9	9	GLFSAIQHK	0.86	0.04
3	HLA-A*11:01	7	15	9	TQLMIQLQK	0.72	0.13
4	HLA-A*11:01	34	42	9	VAIIPALPK	0.64	0.18
5	HLA-A*11:01	3	11	9	STSVLQADK	0.55	0.25

Table 5. MHC I cirA Analysis Results.

No	*Allele*	*Start*	*End*	*Length*	*Peptide*	*Score*	*Percentile Rank*
1	HLA-A*11:01	11	19	9	GVVNIITKK	0.94	0.01
2	HLA-A*11:01	20	28	9	KIVGSPDLK	0.70	0.14
3	HLA-A*11:01	62	70	9	KAYGSLAKR	0.65	0.17
4	HLA-A*11:01	37	45	9	ASSVEQNLK	0.62	0.19
5	HLA-A*11:01	54	62	9	ITQEDLQRK	0.62	0.19

Table 6. MHC I yedX Analysis Results.

No	*Allele*	*Start*	*End*	*Length*	*Peptide*	*Score*	*Percentile Rank*
1	HLA-A*11:01	57	65	9	SQYGYSTYR	0.68	0.16
2	HLA-A*11:01	32	40	9	HILNQQTGK	0.47	0.34
3	HLA-A*11:01	12	20	9	TGDYRVVFK	0.22	0.83
4	HLA-A*11:01	8	16	9	QTATTGDYR	0.20	0.89
5	HLA-A*11:01	42	50	9	HINKVNEHY	0.09	1.5

Table 7. MHC I rbbA Analysis Results.

No	*Allele*	*Start*	*End*	*Length*	*Peptide*	*Score*	*Percentile Rank*
1	HLA-A*11:01	34	42	9	SALSVVREK	0.80	0.08
2	HLA-A*11:01	29	37	9	IIARGTFSK	0.78	0.09
3	HLA-A*11:01	43	51	9	GLLISTFMK	0.46	0.34
4	HLA-A*11:01	60	68	9	GLSILLLKK	0.44	0.38
5	HLA-A*11:01	7	15	9	KLSGGMKQK	0.42	0.39

Table 8. MHC I pykA Analysis Results.

No	*Allele*	*Start*	*End*	*Length*	*Peptide*	*Score*	*Percentile Rank*
1	HLA-A*11:01	19	27	9	AMYAANHLK	0.87	0.04
2	HLA-A*11:01	7	15	9	RVSTFKEGK	0.72	0.13
3	HLA-A*11:01	62	70	9	RTLNLTALY	0.67	0.16
4	HLA-A*11:01	16	24	9	LSNNKGINK	0.64	0.19
5	HLA-A*11:01	29	37	9	LSAEALTEK	0.63	0.19

Table 9. MHC I pykF Analysis Results.

No	*Allele*	*Start*	*End*	*Length*	*Peptide*	*Score*	*Percentile Rank*
1	HLA-A*11:01	19	27	9	QTFTFTTDK	0.86	0.04
2	HLA-A*11:01	48	56	9	FVAASFIRK	0.82	0.07
3	HLA-A*11:01	17	25	9	ALQSGLAHK	0.70	0.14
4	HLA-A*11:01	55	63	9	TAHQLVLSK	0.66	0.16
5	HLA-A*11:01	26	34	9	ASDGIMVAR	0.61	0.21

b. *Salmonella enterica* CT18

The results of the MHC I analysis of *Salmonella enterica* CT18, the pykF protein showed the highest score of 0.86 with the QTFTFTTDK peptide chain, the fepA protein showed the highest score of 0.94 with the GVVNIITKK peptide chain, the sitA protein obtained the highest score of 0.58 with the LALSPAYAK peptide chain, the iroN protein showed the highest score of 0.75 with the YTNYPESSK peptide chain, while the iroB protein obtained the highest score of 0.87 with the VVGPLIAAK peptide chain

Table 10. MHC I pykF Analysis Results.

No	*Allele*	*Start*	*End*	*Length*	*Peptide*	*Score*	*Percentile Rank*
1	HLA-A*11:01	19	27	9	QTFTFTTDK	0.86	0.04
2	HLA-A*11:01	48	56	9	FVAASFIRK	0.82	0.07
3	HLA-A*11:01	17	25	9	ALQSGLAQK	0.73	0.12
4	HLA-A*11:01	26	34	9	ASDGIMVAR	0.61	0.21
5	HLA-A*11:01	25	33	9	IALPALAEK	0.56	0.25

Table 11. MHC I fepA Analysis Results.

No	*Allele*	*Start*	*End*	*Length*	*Peptide*	*Score*	*Percentile Rank*
1	HLA-A*11:01	26	34	9	GVVNIITKK	0.94	0.01
2	HLA-A*11:01	5	13	9	QTNPNYILY	0.69	0.15
3	HLA-A*11:01	12	20	9	NTNTNQLVK	0.60	0.21
4	HLA-A*11:01	56	64	9	LSATWDVTK	0.37	0.47
5	HLA-A*11:01	53	61	9	GLGDDFTLK	0.36	0.49

Table 12. MHC I sitA Analysis Results.

No	*Allele*	*Start*	*End*	*Length*	*Peptide*	*Score*	*Percentile Rank*
1	HLA-A*11:01	19	27	9	LALSPAYAK	0.58	0.22
2	HLA-A*11:01	47	55	9	ITEGPYNGK	0.56	0.23
3	HLA-A*11:01	52	60	9	VTSEGAFSY	0.53	0.27
4	HLA-A*11:01	50	58	9	AAEVSSITK	0.38	0.44
5	HLA-A*11:01	35	43	9	STVSDKPAR	0.37	0.47

Table 13. MHC I iroN Analysis Results.

No	*Allele*	*Start*	*End*	*Length*	*Peptide*	*Score*	*Percentile Rank*
1	HLA-A*11:01	42	50	9	YTNYPESSK	0.75	0.1
2	HLA-A*11:01	2	10	9	TTNRLTSYR	0.68	0.16
3	HLA-A*11:01	22	30	9	GVVNIITKR	0.62	0.19
4	HLA-A*11:01	1	9	9	NSNSNAVTK	0.59	0.22
5	HLA-A*11:01	7	15	9	NVNWTLYGK	0.54	0.26

Table 14. MHC I iroB Analysis Results.

No	*Allele*	*Start*	*End*	*Length*	*Peptide*	*Score*	*Percentile Rank*
1	HLA-A*11:01	42	50	9	VVGPLIAAK	0.87	0.04
2	HLA-A*11:01	34	42	9	ASGGKFAQK	0.82	0.06
3	HLA-A*11:01	54	62	9	AVWEEWWER	0.49	0.3
4	HLA-A*11:01	4	12	9	KSLSNAYRR	0.46	0.34
5	HLA-A*11:01	35	43	9	RGCGIIPGK	0.22	0.82

c. *Proteus mirabilis* HI4320

The results of the MHC I analysis of *Proteus mirabilis* HI4320, PMI2409 protein showed the highest score of 0.96 with the peptide chain ATIRQVAKK, while the ireA protein obtained the highest score of 0.81 with the peptide chain SVYQEQTKR.

Table 15. MHC I PMI2409 Analysis Results.

No	*Allele*	*Start*	*End*	*Length*	*Peptide*	*Score*	*Percentile Rank*
1	HLA-A*11:01	48	56	9	ATIRQVAKK	0.97	0.01
2	HLA-A*11:01	1	9	9	GSQAKIVAK	0.91	0.02
3	HLA-A*11:01	17	25	9	TTAAFHNDK	0.63	0.19
4	HLA-A*11:01	35	43	9	ITRLSTFEK	0.52	0.28
5	HLA-A*11:01	25	33	9	LSAPALTDK	0.48	0.33

Table 16. MHC I ireA Analysis Results.

No	*Allele*	*Start*	*End*	*Length*	*Peptide*	*Score*	*Percentile Rank*
1	HLA-A*11:01	18	26	9	SVYQEQTKR	0.82	0.07
2	HLA-A*11:01	49	57	9	VINKEQLEK	0.79	0.08
3	HLA-A*11:01	7	15	9	FTIKGGIAK	0.77	0.09
4	HLA-A*11:01	45	53	9	KSMSEFTNR	0.76	0.1
5	HLA-A*11:01	11	19	9	NIITKPVTK	0.72	0.12

MHC II

MHC II analysis was performed using the HLA-DRB1*04:01 allele, which is one of the most common alleles in Asian populations. Generally, MHC II epitopes are composed of peptide chains approximately fifteen amino acids long.

a. *Escherichia coli* ATCC 8749

The results of the MHC II analysis of *Escherichia coli* ATCC8739, ECs4935 protein showed the highest score of 0.89 with the RSSFSANINNTAQTN peptide chain, in the cirA protein the highest score was 0.85 with the SGTVTVDTTIQEHRD peptide chain, in the yedX protein the highest score was 0.86 with the DNGWLQLNTAKTDKD peptide chain, the rbbA protein obtained the highest score of 0.94 with the ETRYRYNPDVKSLPA peptide chain, the pykA protein obtained the highest score of 0.80, with the GDKFLLDANLGKGEG peptide chain while the pykF protein obtained the highest score of 0.98 with the TFTFTTDKSVIGNSE peptide chain.

Table 17. MHC II ECs4935Analysis Results.

No	*Allele*	*Start*	*End*	*Length*	*Peptide*	*Score*	*Percentile Rank*
1	HLA-DRB1*04:01	7	21	15	RSSFSANINNTAQTN	0.89	0.26
2	HLA-DRB1*04:01	6	20	15	PRSSFSANINNTAQT	0.84	0.42
3	HLA-DRB1*04:01	10	24	15	DNPRYIAEKNYMEAL	0.82	0.53
4	HLA-DRB1*04:01	9	23	15	TDNPRYIAEKNYMEA	0.79	0.79
5	HLA-DRB1*04:01	11	25	15	NPRYIAEKNYMEALL	0.78	0.87

Table 18. MHC II cirA Analysis Results.

No	*Allele*	*Start*	*End*	*Length*	*Peptide*	*Score*	*Percentile Rank*
1	HLA-DRB1*04:01	25	39	15	SGTVTVDTTIQEHRD	0.85	0.36
2	HLA-DRB1*04:01	24	38	15	WSGTVTVDTTIQEHR	0.77	0.96
3	HLA-DRB1*04:01	26	40	15	DGNVEFAWTPNQNHD	0.70	1.50
4	HLA-DRB1*04:01	25	39	15	IPVFSYYNVNKARIQ	0.69	1.50
5	HLA-DRB1*04:01	26	41	15	SSPITSESNTVDGKY	0.68	1.60

Table 19. MHC II yedX Analysis Results.

No	*Allele*	*Start*	*End*	*Length*	*Peptide*	*Score*	*Percentile Rank*
1	HLA-DRB1*04:01	54	68	15	DNGWLQLNTAKTDKD	0.86	0.31
2	HLA-DRB1*04:01	18	32	15	PSLVYAAQQNILSVH	0.84	0.41
3	HLA-DRB1*04:01	19	33	15	SLVYAAQQNILSVHI	0.81	0.58
4	HLA-DRB1*04:01	53	67	15	ADNGWLQLNTAKTDK	0.79	0.80
5	HLA-DRB1*04:01	38	52	15	PVEFHINKVNEHYHV	0.79	0.81

Table 20. MHC II rbbA Analysis Results.

No	*Allele*	*Start*	*End*	*Length*	*Peptide*	*Score*	*Percentile Rank*
1	HLA-DRB1*04:01	702	716	15	ETRYRYNPDVKSLPA	0.94	0.09
2	HLA-DRB1*04:01	701	715	15	IETRYRYNPDVKSLP	0.92	0.17
3	HLA-DRB1*04:01	55	69	15	IPPYQPENAEIAIEA	0.84	0.44
4	HLA-DRB1*04:01	265	279	15	NIETRYRYNPDVKSL	0.84	0.44
5	HLA-DRB1*04:01	700	714	15	TRYRYNPDVKSLPAI	0.82	0.53

Table 21. MHC II pykA Analysis Results.

No	*Allele*	*Start*	*End*	*Length*	*Peptide*	*Score*	*Percentile Rank*
1	HLA-DRB1*04:01	21	35	15	GDKFLLDANLGKGEG	0.80	0.71
2	HLA-DRB1*04:01	3	17	15	VTPVHFDSANDGVAA	0.77	0.90
3	HLA-DRB1*04:01	20	34	15	IGDKFLLDANLGKGE	0.74	1.10
4	HLA-DRB1*04:01	4	18	15	TPVHFDSANDGVAAA	0.70	1.40
5	HLA-DRB1*04:01	5	19	15	PVHFDSANDGVAAAS	0.70	1.50

Table 22. MHC II pykF Analysis Results.

No	*Allele*	*Start*	*End*	*Length*	*Peptide*	*Score*	*Percentile Rank*
1	HLA-DRB1*04:01	20	34	15	TFTFTTDKSVIGNSE	0.98	0.01
2	HLA-DRB1*04:01	19	33	15	QTFTFTTDKSVIGNS	0.96	0.04
3	HLA-DRB1*04:01	37	51	15	VRKYFPDATILALTT	0.95	0.06
4	HLA-DRB1*04:01	36	50	15	AVRKYFPDATILALT	0.94	0.09
5	HLA-DRB1*04:01	21	35	15	FTFTTDKSVIGNSEM	0.92	0.17

b. *Salmonella enterica* ATCC8739

The results of the MHC II analysis of *Salmonella enterica* CT18, the pykF protein showed the highest score of 0.98 with the peptide chain TFTFTTDKSVVGNNE, the fepA protein showed the highest score of 0.91 with the peptide chain TDVYQWENVPKAVVE, the sitA protein obtained the highest score of 0.92 with the peptide chain DALVKYDPDNAQIYK, the iroN protein showed the highest score of 0.96 with the peptide chain GETIVVESTAEQVLK, while the iroB protein obtained the highest score of 0.70 with the peptide chain EAGLVVFDAAPGFDS.

Table 23. MHC II pykF Analysis Results.

No	*Allele*	*Start*	*End*	*Length*	*Peptide*	*Score*	*Percentile Rank*
1	HLA-DRB1*04:01	20	34	15	TFTFTTDKSVVGNNE	0.98	0.01
2	HLA-DRB1*04:01	19	33	15	QTFTFTTDKSVVGNN	0.97	0.02
3	HLA-DRB1*04:01	37	51	15	VRKYFPDATILALTT	0.95	0.06
4	HLA-DRB1*04:01	36	50	15	AVRKYFPDATILALT	0.94	0.09
5	HLA-DRB1*04:01	21	35	15	FTFTTDKSVVGNNEI	0.93	0.13

Table 24. MHC II fepA Analysis Results.

No	*Allele*	*Start*	*End*	*Length*	*Peptide*	*Score*	*Percentile Rank*
1	HLA-DRB1*04:01	17	31	15	TDVYQWENVPKAVVE	0.91	0.18
2	HLA-DRB1*04:01	54	68	15	RLGWRGERDTRGDTA	0.88	0.26
3	HLA-DRB1*04:01	16	30	15	KTDVYQWENVPKAVV	0.87	0.28
4	HLA-DRB1*04:01	30	44	15	PKKYDYQGNPVTGTD	0.86	0.31
5	HLA-DRB1*04:01	53	67	15	VRLGWRGERDTRGDT	0.83	0.44

Table 25. MHC II sitA Analysis Results.

No	*Allele*	*Start*	*End*	*Length*	*Peptide*	*Score*	*Percentile Rank*
1	HLA-DRB1*04:01	6	20	15	DALVKYDPDNAQIYK	0.92	0.17
2	HLA-DRB1*04:01	5	19	15	RDALVKYDPDNAQIY	0.86	0.33
3	HLA-DRB1*04:01	28	42	15	IPAIFSESTVSDKPA	0.80	0.64
4	HLA-DRB1*04:01	7	21	15	ALVKYDPDNAQIYKQ	0.80	0.74
5	HLA-DRB1*04:01	27	41	15	KEKFKVITTFTVIAD	0.74	1.10

Table 26. MHC II iroN Analysis Results.

No	*Allele*	*Start*	*End*	*Length*	*Peptide*	*Score*	*Percentile Rank*
1	HLA-DRB1*04:01	31	45	15	GETIVVESTAEQVLK	0.96	0.04
2	HLA-DRB1*04:01	55	69	15	EAGYSRQGNIYAGDT	0.93	0.13
3	HLA-DRB1*04:01	54	68	15	FEAGYSRQGNIYAGD	0.92	0.18
4	HLA-DRB1*04:01	29	43	15	DNGETIVVESTAEQV	0.92	0.18
5	HLA-DRB1*04:01	30	44	15	NGETIVVESTAEQVL	0.91	0.18

Table 27. MHC II iroB Analysis Results.

No	*Allele*	*Start*	*End*	*Length*	*Peptide*	*Score*	*Percentile Rank*
1	HLA-DRB1*04:01	45	59	15	EAGLVVFDAAPGFDS	0.70	1.50
2	HLA-DRB1*04:01	44	58	15	AEAGLVVFDAAPGFD	0.62	1.90
3	HLA-DRB1*04:01	15	29	15	LISWVMDSASEVDAE	0.50	3
4	HLA-DRB1*04:01	46	60	15	AGLVVFDAAPGFDSE	0.44	3.70
5	HLA-DRB1*04:01	14	28	15	DLISWVMDSASEVDA	0.38	4.60

c. *Proteus mirabilis* HI4320

The results of the MHC I analysis of *Proteus mirabilis* HI4320, PMI2409 protein showed the highest score of 0.95 with the peptide chain PVTYQRQNNNDGDEN, while in the ireA protein the highest score was obtained at 0.93 with the peptide chain LKLYQYDNVGKANIK.

Table 28. MHC II PMI2409 Analysis Results.

No	*Allele*	*Start*	*End*	*Length*	*Peptide*	*Score*	*Percentile Rank*
1	HLA-DRB1*04:01	2	16	15	PVTYQRQNNNDGDEN	0.95	0.08
2	HLA-DRB1*04:01	1	15	15	TPVTYQRQNNNDGDE	0.93	0.13
3	HLA-DRB1*04:01	48	62	15	NNNIYALTDNPALAG	0.91	0.18
4	HLA-DRB1*04:01	47	61	15	PNNNIYALTDNPALA	0.88	0.27
5	HLA-DRB1*04:01	17	31	15	GDSFILNADLDSTQG	0.87	0.28

Table 29. MHC II ireA Analysis Results.

No	*Allele*	*Start*	*End*	*Length*	*Peptide*	*Score*	*Percentile Rank*
1	HLA-DRB1*04:01	25	39	15	LKLYQYDNVGKANIK	0.93	0.13
2	HLA-DRB1*04:01	24	38	15	GLKLYQYDNVGKANI	0.88	0.26
3	HLA-DRB1*04:01	35	49	15	KANIKGIETAVAFPV	0.88	0.26
4	HLA-DRB1*04:01	26	40	15	KLYQYDNVGKANIKG	0.88	0.26
5	HLA-DRB1*04:01	43	57	15	NRDLKPETSVSQEIG	0.88	0.27

Subcellular Location Analysis Results

Analysis of the subcellular location of proteins in *Escherichia coli* ATCC8739, *Salmonella enterica* CT18, and *Proteus mirabilis HI4320* that interact with EGCG was performed using PSORTb v3.0 via the website https://www.psort.org/psortb/ , with a focus on virulent proteins. The analysis results showed that the virulent proteins from the three bacteria have different subcellular locations, even among proteins within the bacteria.

Table 30. Results of Subcellular Location Analysis of Virulent Proteins of *Escherichia coli* ATCC8739.

Organism	Identifier	Functional Proteins	Subcellular Location
Escherichia coli ATCC8739	ECs4935	ShET2 enterotoxin domain-containing protein	*Unknown*
	cirA	colicin I receptor	*Outer Membrane*
	yedX	hydroxyisourate hydrolase	*Unknown*
	rbbA	ABC transporter-like protein	*Cytoplasmic Membrane*
	pykA	pyruvate kinase	*Cytoplasmic*
	pykF	pyruvate kinase	*Cytoplasmic*

Based on the results of the subcellular location of the virulent protein of *Escherichia coli* ATCC8739, the cirA protein was found to be subcellularly located in the outer membrane, the pykA and pykF proteins were found in the cytoplasm, the rbbA protein was found in the cytoplasmic membrane, and ECs4935 and yedX were found to be unknown because they did not have characteristic sequences or conservative motifs that could be recognized by PSORTb.

Table 31. Results of Subcellular Location Analysis of Virulent Proteins of *Salmonella enterica* CT18.

Organism	Identifier	Functional Proteins	Subcellular Location
Salmonella enterica CT18	pykF	pyruvate kinase	*Cytoplasmic*
	fepA	outer membrane receptor FepA	*Outer Membrane*
	sitA	Iron transport protein periplasmic-binding protein	*Periplasmic*
	iroN	outer membrane receptor FepA	*Outer Membrane*
	iroB	glycosyltransferase	*Unknown*

Based on the results of the subcellular location of the *Salmonella enterica* CT18 virulent protein, the pykF protein was found to be subcellularly located in the cytoplasm, the fepA and iroN proteins were located in the outer membrane, the sitA protein was located in the periplasm, and iroB was found to be unknown because it did not have a characteristic sequence or conservative motif that could be recognized by PSORTb.

Table 31. Results of Subcellular Location Analysis of Virulent Proteins of *Proteus mirabilis* HI4320.

Organism	Identifier	Functional Proteins	Subcellular Location
Proteus mirabilis HI4320	PMI2409	outer membrane receptor	*Cytoplasmic*
	ireA	iron-regulated outer membrane virulence protein	*Outer Membrane*

Based on the results of the subcellular location of the virulent protein *Proteus mirabilis* HI4320, the PMI2409 protein was found to be subcellularly located in the cytoplasm, and ireA was found in the outer membrane.

Discussion

The bioinformatics approach in this study played a crucial role in predicting the molecular interactions between luteolin and virulence factor proteins from *Escherichia coli* ATCC8739, *Salmonella enterica* CT18, and *Proteus mirabilis* HI4320, three Gram-negative bacteria involved in gastrointestinal infections. This method enabled the efficient identification of potential targets without the need for time-consuming and costly preliminary experimental testing. This type of analysis enabled the identification of potential targets through the integration of protein chemistry data as implemented in the STITCH v5.0 database (Szklarczyk et al., 2016). Through the combination of VICMPred, VirulentPred, BepiPred, MHC BindingPred, and PSORTb tools, a comprehensive picture of protein chemistry interactions, functional classification, immunogenic epitope prediction, and protein subcellular location was obtained. This microbioinformatics approach is now an important foundation in the exploration of natural antimicrobial agent candidates because it can link molecular data with bacterial virulence and resistance mechanisms (Zhang et al., 2025).

STITCH analysis produces interaction network visualizations that depict the relationships between compounds and proteins using two main elements: nodes and edges. Nodes are divided into two categories: compound nodes and protein nodes. Red or orange nodes represent the chemical compounds of interest and are typically accompanied by a molecular structure icon to distinguish them from proteins. Other colored nodes, such as green, blue, or purple, represent proteins predicted to have a functional relationship with the compound. Node size also provides important information: nodes displaying a structure icon within a circle indicate that the protein has 3D structure data that has been characterized in databases such as PDB or AlphaFold, and are therefore depicted as larger nodes. Nodes without an icon represent proteins for which incomplete structural information is available or are still uncharacterized, and are displayed as smaller nodes. Relationships between nodes are represented by edges, where the thickness and length of the lines indicate the strength of the interaction; thicker and shorter edges indicate stronger associations, while thinner and longer edges indicate weaker associations. Overall, the configuration of nodes and edges in STITCH provides a comprehensive picture of the interaction patterns between compounds and proteins, making it easier to understand the potential working mechanisms of compounds on the biological systems being analyzed.

STITCH is a database used to predict and visualize the relationship between chemical compounds and proteins, including functional linkage patterns and potential interactions. Through analysis using STITCH v5.0 by entering the keyword "luteolin" and each bacterial species, a list of proteins that appear as candidate interaction targets was obtained. In *Escherichia coli* ATCC8739, *Salmonella enterica* CT18, and *Proteus mirabilis* HI4320, using STITCH v5.0 from each bacterium, ten proteins were found to appear after being targeted by luteolin. In *Escherichia coli* ATCC8739, ten interacting proteins were found, namely ECs4935, yahD, fepA, cirA, yedX, rbbA, pykA, pykF, htpG, and nudH. In *Salmonella enterica* CT18, ten interacting proteins were identified: STY4224, pykF, hiuH, pykA, htpG, fepA, sitA, iroN, iroB, and rppH. In *Proteus mirabilis* HI4320, ten interacting proteins were identified: PMI2409, htpG, rppH, PMI1224, pykA, pykF, PMI0842, cysj, ireA, and sitA. Each protein has a distinct identification code and exhibits a specific functional relationship with luteolin. A closer examination of the interaction network revealed that some proteins not only interact with luteolin but also interact with each other, indicating a synchrony of biological functions. Protein selection was based on a specific cut-off value, ensuring that the proteins identified were strong candidates relevant to the mechanism of luteolin action on the bacteria (Szklarczyk et al., 2016).

Analysis using VICMpred and VirulentPred was conducted to identify virulent proteins based on their cellular function and role in bacterial metabolism. These two methods were selected based on their ability to distinguish virulent proteins from housekeeping proteins through sequence motif analysis and biochemical properties. VICMpred classifies proteins into four main functional categories: cellular process, metabolic molecule, information and storage, and virulence factors (Saha et al., 2006). Meanwhile, VirulentPred predicts virulence potential based on a Support Vector Machine (SVM) algorithm trained with experimental data from pathogenic bacteria (Garg et al., 2008).

Based on data obtained from VICMpred, virulent proteins can be grouped. In *Escherichia coli* ATCC8739, ECs4935 (ShET2 enterotoxin domain-containing protein), cirA (colicin I receptor), yedX (hydroxyisourate hydrolase), rbbA (ABC transporter-like protein), pykA,

and pykF (pyruvate kinase) were found. In *Salmonella enterica* CT18, pykF (pyruvate kinase), fepA and iroN (outer membrane receptor FepA), sitA (Iron transport protein periplasmic-binding protein), and iroB (glycosyltransferase) were found. In *Proteus mirabilis* HI4320, ireA (iron-regulated outer membrane virulence protein) and PMI2409 (pyruvate kinase) were found (Saha et al., 2006).

The results of the VICMpred functional class show differences in the distribution of protein functions in the three bacterial species. In *Escherichia coli* ATCC8739, the ECS4935, cirA, and yedX proteins are involved in cellular processes that support membrane transport and cell wall stability, thus playing a role in maintaining integrity during mucosal colonization (Pakbin et al., 2021). The rbbA and pykF proteins are categorized as metabolic molecules that support ribosome translocation and the glycolysis pathway to maintain energy balance, while pykA, as a virulence factor, acts as a metabolic sensor that connects glycolysis with cellular activity during infection (Horemans et al., 2022). The combined activity of these transport, metabolic, and energy proteins strengthens *E. coli*'s ability to survive in an intestinal environment rich in oxidative stress, and luteolin is thought to suppress these functions through inhibition of the metal transport system and disruption of cellular energy balance.

In *Salmonella enterica* CT18, pykF and sitA are metabolic molecules that maintain energy efficiency and metal homeostasis, while FepA and iroN, classified as virulence factors, play a role in the salmochelin–enterobactin siderophore system for iron uptake during infection (Cunrath et al., 2021). The iroB protein, which is involved in cellular processes, supports siderophore modification and cell wall stability against oxidative stress. In *Proteus mirabilis* HI4320, ireA is a virulence factor that acts as the primary adhesin mediating bacterial adhesion to the gastrointestinal epithelium, while PMI2409 is a metabolic molecule that functions in adaptive metabolism that enables colonization in the mucosal environment (Chakkour et al., 2024). This combination of roles suggests that virulence factors work in coordination with metabolic activity and metal transport to support colonization. Luteolin has the potential to suppress these mechanisms by binding to siderophore receptor domains and metabolic enzymes, thereby inhibiting iron acquisition, epithelial adhesion, and bacterial energy efficiency without disrupting host cells.

VirulentPred predicts the virulence potential of proteins based on their amino acid composition and dipeptide pattern. A positive score indicates a protein's propensity for virulent activity, while a negative score indicates non-virulence. In this analysis, a value >0.0 is used as a practical confidence limit for classifying proteins with high virulence potential (Garg et al., 2008). Proteins with scores below this threshold generally play a role in basic cellular functions not directly related to pathogenesis, such as yahD, htpG, and nudH. The analysis focused on proteins with biological relevance to gastrointestinal virulence mechanisms, such as iron uptake and mucosal adhesion, as these proteins are most relevant to luteolin's mechanism of action (Garg et al., 2008).

In *Escherichia coli* ATCC8739, the cirA protein functions as a TonB-dependent receptor that facilitates iron uptake through a Fe^{3+} complex with a catecholate siderophore, thus supporting bacterial survival and colonization in the gastrointestinal tract. The ECs4935 protein plays a role in colonization of the intestinal mucosa and has pathogenic characteristics that support the infectious ability of *E. coli* (Pakbin et al., 2021). Related proteins rbbA, pykA, and pykF contribute to energy metabolism and cellular redox balance that support bacterial survival during gastrointestinal infection, although not directly related to the main virulence mechanism (Ding et al., 2024). In *Salmonella enterica* CT18, the combination of fepA, sitA, iroN, and iroB proteins forms a complex siderophore system that plays an important role in iron transport and modification during gastrointestinal infection. TonB-dependent receptors such as fepA and iroN enable iron uptake under conditions of metal deficiency, which is one of the key mechanisms of *S. enterica* colonization and virulence (Cunrath et al., 2021), sitA acts as an Fe^{2+}/Mn^{2+}-binding protein in the sitABCD transporter system that supports metal uptake during iron deficiency conditions, while iroB is a C-glycosyltransferase that modifies enterobactin into salmochelin as the main siderophore in the process of iron acquisition and virulence (Singh et al., 2023; Mohsen et al., 2023). In *Proteus mirabilis* HI4320, the ireA protein functions as the main adhesin that mediates attachment to the epithelium of the digestive tract, in addition, the results of the bioinformatics analysis of this study also indicate that the PMI2409 protein has the potential to play a role in adaptive metabolism that supports the colonization process (Chakkour et al., 2024).

Mechanistically, the protein target pattern identified in this study is consistent with various other studies on luteolin, although using different methods. In vitro research by Ding. showed that luteolin isolated from Lophatherum gracile in multiresistant *E. coli* was able to damage cell walls and membranes, increase cell content leakage, reduce ATP synthesis, and alter the expression of proteins related to energy metabolism and stress responses. The research by Mahamud. was an in vitro study that tested the antibacterial activity of luteolin against Salmonella Typhimurium and *Escherichia coli*. The results showed that luteolin had strong antibacterial activity in vitro, indicated by a decrease in MIC and MBC values in both test bacteria. Luteolin was also shown to significantly inhibit biofilm formation, reduce the ability of bacterial cell adhesion to biotic and abiotic surfaces, and cause damage to the outer and inner membranes of bacteria, indicated by increased

permeability and cell content leakage. Luteolin decreased ATP production and energy metabolism activity, indicating that this compound not only damages cell structure but also disrupts the physiological functions of bacteria. Overall, these in vitro findings strengthen the hypothesis that luteolin works through a combination of mechanisms including membrane damage, adhesion disruption, biofilm inhibition, and energy metabolism disruption (Mahamud et al., 2024).

Based on a literature review conducted by Wasfi, *Proteus mirabilis* possesses various important virulence factors such as biofilm formation, swarming motility, and the expression of various surface proteins that support colonization and increase its resistance to antimicrobial therapy. This is in line with in vitro findings by Alamuri which showed that trimeric autotransporters play a direct role in adhesion, invasion, and agglutination processes, thus being a key component in the early stages of infection. Both studies confirmed that surface proteins have a significant contribution to the virulence of *P. mirabilis*, and therefore have the potential to be targets for intervention by antibacterial compounds such as luteolin, which is known to inhibit various virulence mechanisms in pathogenic bacteria (Wasfi et al., 2020; de Nies et al., 2021).

This VICMpred and VirulentPred study found discrepancies between functional class and virulence analysis. Several proteins, such as pykA in *Salmonella enterica* CT18 and PMI0842, sysJ, and sitA in *Proteus mirabilis* HI4320, were predicted as functionally virulence factors by VICMpred, but were assessed as non-virulent by VirulentPred. This difference does not necessarily indicate that one method is more accurate, but rather reflects the differences in the approaches and analytical principles used. VirulentPred assesses virulence potential based on dipeptide patterns and sequence features commonly found in active virulent proteins, while VICMpred assesses a protein's biological function more broadly based on conservative motifs and functional categories. Therefore, VirulentPred results serve as the primary basis in this study for assessing the virulence potential of target proteins, while VICMpred results are used to strengthen biological interpretations for a more comprehensive understanding. Similar findings were also reported by de Nies, who emphasized the importance of integration between computational predictions and biological analysis in the validation of virulence factors (de NIies et al., 2024).

A total of 13 proteins consisting of *Escherichia coli* ATCC8739 (ECs4935, cirA, yedX, rbbA, pykF, and pykA), *Salmonella enterica* CT18 (pykF, sitA, fepA, iroN, and IroB), and *Proteus mirabilis* HI4320 (sitA and PMI2409) were identified as virulence factors from the results of virulence property analysis and then continued with linear B cell epitope mapping in virulent *E. coli*, *S. enterica*, and *P. mirabilis* bacteria using BepiPred v1.0. The analysis was carried out with a default threshold value of 0.350. This value is used as a determining limit to distinguish immunogenic and non-immunogenic residues, where residues with a score ≥ 0.350 are categorized as potential linear epitope candidates, while residues with a value below the threshold are considered non-immunogenic. A score above the threshold indicates that the protein fragment is hydrophilic, flexible, and surface-exposed, which are important characteristics for an epitope to be recognized by an antibody.63 Identification of B-cell epitopes is a fundamental step for the development of epitope-based vaccines, therapeutic antibodies, and diagnostic tools (Potocnakova et al., 2061).

Based on the analysis of the B cell epitope prediction graph, it shows that in the virulent proteins of three bacteria, namely the cirA protein in *Escherichia coli* ATCC8739, fepA and iroN in *Salmonella enterica* CT18, and ireA in *Proteus mirabilis* HI4320, the highest and widest fragments above the threshold value (threshold ≥ 0.350) are on surface proteins related to iron uptake or adhesion, thus displaying the highest immunogenic potential. For example, tonB-dependent transporters such as fepA and IroN have been proven to be vaccine candidates in Gram-negative bacteria because their expression on the cell surface allows antigen exposure to the immune system (Wang et al., 2021). The more and wider the peaks in the graph above the threshold reflect fragments that have a greater chance of being recognized by antibodies and forming a protective humoral response, making these proteins the main targets in the development of epitope-based subunit vaccines.

The proteins of the three virulent bacteria were also analyzed for MHC I and MHC II using MHC I Binding Predictions and MHC II Binding Predictions. MHC I analysis focuses on peptide chains capable of binding to cytotoxic T cells. The results of the MHC I analysis obtained several peptide chains capable of binding to cytotoxic T cells complete with scores and rankings. The selection of the HLA-A*11:01 allele in the T cell class I epitope analysis was based on biological and demographic reasons, because this allele has a high frequency in Southeast Asian populations with a prevalence of around 24.5%, making it a very representative allele for use in immunoinformatics analysis (Habel et al., 2022). This study selected the five peptides with the highest scores from the prediction results because these fragments represent candidates with the strongest binding affinity and the greatest opportunity to be presented by MHC I on the cell surface and recognized by $CD8^+$ T cells, which can then elicit a protective immune response.

The highest value in the top five rankings of each protein interacting with the luteolin compound indicates the potential for strong binding between the epitope and the protein, with the involvement of individual alleles as an important indicator in the development of T cell-based immunological therapeutic agents. This finding confirms

that the prediction of MHC class I epitopes plays a role in designing specific adaptive immune responses to pathogens while also being able to coordinate with the recognition of B cell epitopes (Tadros et al., 2025). The strength of the interaction is reflected in the relationship between the percentile rank and score values, where the better the binding performance will result in a smaller percentile rank and a higher score, indicating dominant binding to the MHC I allele HLA-A*11:01.

The next analysis was performed using MHC class II to identify peptide fragments from virulent proteins that could potentially be recognized by helper T cells ($CD4^+$). The MHC II pathway plays a crucial role in activating the adaptive immune system, particularly in stimulating B cells to produce antibodies and regulating cytokine secretion, which enhances communication between immune cells. This approach illustrates the principle of efficiency in immunoinformatics, where epitopes with the highest affinity scores are considered most likely to form stable peptide–MHC II complexes, thus optimally triggering $CD4^+$ cell activation (Tadros et al., 2020). Based on the prediction results, the five peptides with the highest affinity scores and the lowest percentile rank for each virulent protein were selected because they demonstrated the formation of the most stable peptide–MHC II complexes and were most likely to be recognized by the $CD4^+$ receptor. This correlation indicates that the higher the score, the stronger the binding ability, thus increasing the likelihood of T helper cell activation (Reynisson et al., 2020; Jensen et al., 2018).

Overall, the analysis of MHC class I and MHC class II in this study indicates two distinct but complementary mechanisms in the adaptive immune response. MHC class I plays a role in the presentation of endogenous peptides from intracellular proteins and is recognized by cytotoxic T cells ($CD8^+$), which function to destroy bacterially infected cells. MHC class II presents exogenous peptides from surface proteins or bacterial secretions to be recognized by helper T cells ($CD4^+$), which then activate B cells and increase cytokine secretion to form a humoral immune response (Wieczorek et al., 2017). MHC class I illustrates the potential of each protein in stimulating the cellular immune pathway through the activation of cytotoxic T cells ($CD8^+$), while MHC class II emphasizes its role in supporting the humoral immune pathway by triggering the activation of helper T cells ($CD4^+$) that play a role in B cell stimulation and cytokine secretion.

PSORTb is used to predict the subcellular location of virulence proteins in *Escherichia coli* ARCC8739, *Salmonella enterica* CT18, and *Proteus mirabilis* HI4320, in order to understand the relationship between the functional position of the protein and the potential interaction of the luteolin compound. This tool has a high level of accuracy in mapping protein locations in Gram-negative bacteria because it combines analysis of signal peptides, transmembrane domains, and conserved motifs that indicate the unique characteristics of each cell compartment (Venus et al., 2021). The subcellular location of three virulent proteins was found in three different locations, namely the outer membrane, cytoplasmic membrane, cytoplasmic, and periplasmic, and there were three proteins that were found to be unknown. Each location determines the role and mechanism carried out by the protein in supporting a bacterium's virulence strategy.

Based on the results of PSORTb analysis, the CirA protein in *Escherichia coli* is predicted to be located on the outer membrane, making it highly relevant to the mechanism of luteolin, which is known to damage the bacterial outer wall and membrane, increasing permeability, and causing leakage of cell contents (Ding et al., 2024). This outer membrane damage has the potential to disrupt the stability and function of cirA as a TonB-dependent receptor in iron uptake. The rbbA protein in *Escherichia coli* ATCC8739 is located on the cytoplasmic membrane and plays a role in membrane transport processes that require membrane structure stability and cellular energy support. The function of membrane proteins is strongly influenced by the physical state of the membrane because transport and bioenergetic activity depend on membrane integrity as a selective boundary that regulates the movement of substances between cell compartments. Luteolin activity, which has been shown to increase cytoplasmic membrane permeability and damage bacterial membrane structures, has the potential to reduce the efficiency of rbbA through disruption of membrane stability and changes in physiological conditions that affect the transport process (How et al., 2024). The pykA and pykF proteins are located in the cytoplasm as glycolysis enzymes. The mechanism of luteolin, which includes decreased ATP levels, impaired cellular respiration, and metabolic stress, allows for a decrease in the activity of the cytoplasmic enzyme due to limited intracellular energy (Guo et al., 2020). The yedX and ECs4935 proteins are categorized as unknown because they do not have characteristic sequences or conserved motifs that can be recognized by PSORTb, such as signal peptides, transmembrane domains, or well-defined subcellular localization motifs. These two proteins are classified as hypothetical proteins with functions that have not been characterized experimentally, so the PSORTb algorithm cannot determine their subcellular location with certainty (Venus et al., 2021). Further research exploration is recommended.

In *Salmonella enterica* CT18, PSORTb predicts that fepA and iroN are located in the outer membrane, so these proteins have the potential to experience structural disruption when luteolin damages the outer membrane layer, because flavonoids including luteolin have been reported to be able to change the fluidity and stability of the outer membrane of Gram-negative bacteria (Bunea et al., 2025). The pykF protein is located in the cytoplasm and functions as a pyruvate kinase that carries out the

final stage of glycolysis to produce ATP. Because it is a metabolic enzyme, its activity is highly dependent on intracellular energy stability. Luteolin itself does not directly target pykF, but research shows that luteolin can disrupt energy homeostasis and reduce cellular ATP production capacity, so these altered cytoplasmic conditions have the potential to indirectly inhibit the activity of metabolic enzymes, including pykF (Guo et al., 2020). The sitA protein, which is located in the periplasm, is part of the SitABCD transporter system that plays a role in binding and transporting Mn^{2+} and Fe^{2+} ions, which are important for metal homeostasis and Salmonella's resistance to oxidative stress. The sitA protein, located in the periplasmic space, functions highly dependent on the integrity of the outer membrane. The mechanism of action of luteolin, which is capable of damaging the outer membrane, increasing permeability, and causing leakage of cellular components, can disrupt periplasmic conditions, thereby inhibiting sitA's ability to bind essential metal ions (Uppalapati et al., 2022). The iroB protein is categorized as unknown because it does not have a characteristic transmembrane domain or signal peptide that can be identified by PSORTb, although it is known to play a role in the glycosylation process of salmochelin as a siderophore modification enzyme (Venus et al., 2021).

In *Proteus mirabilis* HI4320, the PMI2409 protein is predicted by PSORTb to be located in the cytoplasm, so its function is related to metabolic processes and intracellular energy regulation. Cytoplasmic proteins are highly dependent on the stability of cellular energy, so the effects of luteolin in the form of decreased ATP, induction of metabolic stress, and disruption of ionic homeostasis can reduce the activity of cytoplasmic proteins including PMI2409 indirectly through reduced energy and changes in the physiological conditions of the cell (Chakkour et al., 2024; Venus et al., 2021). The ireA protein is predicted to be localized on the outer membrane and functions as an adhesin that helps *P. mirabilis* adhere to the surface of the mucosal epithelium. This location makes the ireA protein easily accessible to external molecules such as luteolin, which can potentially interact and reduce adhesion activity, thereby inhibiting biofilm formation and bacterial colonization in host tissues (Armbruster et al., 2017).

CONCLUSIONS

Luteolin has been shown to interact with various virulence proteins in *Escherichia coli* ATCC8739, *Salmonella enterica* CT18, and *Proteus mirabilis* HI4320. In *Escherichia coli* ATCC8739, luteolin targets cirA, ECs4935, yedX, rbbA, pykA, and pykF, which play a role in iron uptake, membrane stability, mucosal colonization, and energy metabolism. In *Salmonella enterica* CT18, luteolin interacts with fepA, iroN, iroB, sitA, and pykF, which are components of the salmochelin–enterobactin siderophore system, periplasmic Fe^{2+}/Mn^{2+} transport, and the glycolysis pathway, which are important for bacterial growth and adaptation during infection. In *Escherichia coli* ATCC8739, luteolin is predicted to target ireA and PMI2409, which play a role in epithelial adhesion, Fe/Mn homeostasis, and adaptive metabolism. Overall, this interaction pattern suggests that luteolin works primarily by inhibiting the iron uptake system, disrupting energy metabolism, and inhibiting bacterial adhesion, thereby reducing the ability of all three bacteria to colonize and survive in the host environment.

Acknowledgements: The authors are greatful to academic mentors from the Departement of Microbioilogy and the Departement of Pharmacology, Faculty of Medicine, Universitas Palangka Raya, for their guidance and support throughout the development and preparation of this manuscript

Authors' Contributions: Syamsuddin M.S.R., Praja R.K and Nawan. Conceived the study and undertook the literarture review.Syamsuddin M.S.R, independently and in collaboration with Praja R.K., executed the bioinformatic analysis. Teresa A and Frethernety A., reviewed the manuscript and provided essential revisions prior to approval of the final version for publication

Competing Interests: The authors declare that there are no competing interests.

Funding: The authors declare no external funding for the study

REFERENCES

Alamuri P, Löwer M, Hiss JA, Himpsl SD, Schneider G, Mobley HLT. Adhesion, invasion, and agglutination mediated by two trimeric autotransporters in the human uropathogen *Proteus mirabilis*. Infect Immun [Internet]. 2010 Nov [cited 2025 Nov 19];78(11):4882–94. Available from: /doi/pdf/10.1128/iai.00718-10?download=true

Amanda AC, Khairunnisa, Hrp AFM, Syamputra RM, Hrp AAN, Tambunan Nurhasanah, et al. View of Masa Depan Bio Informatika : Mengubah Data Menjadi Terapi. 2025 [cited 2025 May 6];3:17–23. Available from: https://ifrelresearch.org/index.php/jusiik-widyakarya/article/view/4410/4594

Armbruster CE, Mobley HLT, Pearson MM. Pathogenesis of *Proteus mirabilis* Infection. EcoSal Plus [Internet]. 2018 Dec 31 [cited 2025 Nov 9];8(1):10.1128/ecosalplus.ESP-0009–2017. Available from: https://pmc.ncbi.nlm.nih.gov/articles/PMC5880328/.

Bunea A, Cenariu MC, Andrei S, De Rossi L, Rocchetti G, Lucini L, et al. Antimicrobial Potential of Polyphenols: Mechanisms of Action and Microbial Responses—A Narrative Review. Antioxidants 2025, Vol 14, Page 200 [Internet]. 2025 Feb 10

[cited 2025 Nov 17];14(2):200. Available from: https://www.mdpi.com/2076-3921/14/2/200/htm

Campos J, Mourão J, Peixe L, and Antunes P. Non-typhoidal salmonella in the pig production chain: A comprehensive analysis of its impact on human health. Pathogens [Internet]. 2019 [cited 2025 May 20];8(1). Available from: https://pubmed.ncbi.nlm.nih.gov/30700039/.

Chagas SSM, Behrens MD, Moragas-Tellis JC, Penedo GXM, Silva AR, and Gonçalves-De-Albuquerque FC. Flavonols and Flavones as Potential anti-Inflammatory, Antioxidant, and Antibacterial Compounds. Vol. 2022, Oxidative Medicine and Cellular Longevity. Hindawi Limited; 2022.

Chakkour M, Hammoud Z, Farhat S, El Roz A, Ezzeddine Z, Ghssein G. Overview of *Proteus mirabilis* pathogenicity and virulence. Insights into the role of metals. Front Microbiol. 2024 Apr 5;15:1383618.

Cunrath O, Palmer JD. An overview of *Salmonella enterica* metal homeostasis pathways during infection. microLife [Internet]. 2021 Dec 15 [cited 2025 Nov 2];2. Available from: https://dx.doi.org/10.1093/femsml/uqab001

de Nies L, Lopes S, Busi SB, Galata V, Heintz-Buschart A, Laczny CC, et al. PathoFact: a pipeline for the prediction of virulence factors and antimicrobial resistance genes in metagenomic data. Microbiome 2021 9:1 [Internet]. 2021 Feb 17 [cited 2025 Nov 6];9(1):1–14. Available from: https://microbiomejournal.biomedcentral.com/articles/10.1186/s40168-020-00993-9

Ding Y, Wen G, Wei X, Zhou H, Li C, Luo Z, et al. Antibacterial activity and mechanism of luteolin isolated from Lophatherum gracile Brongn. against multidrug-resistant *Escherichia coli*. Front Pharmacol. 2024 Jun 24;15:1430564.

El-Rami EF, and Sikora EA. Bioinformatics Workflow for Gonococcal Proteomics. In: Methods in Molecular Biology. Humana Press Inc.; 2019. p. 185–205.

Garg A, Gupta D. VirulentPred: a SVM based prediction method for virulent proteins in bacterial pathogens. BMC Bioinformatics 2008 9:1 [Internet]. 2008 Jan 28 [cited 2025 Oct 30];9(1):1–12. Available from: https://bmcbioinformatics.biomedcentral.com/articles/10.1186/1471-2105-9-62.

Guo Y, Liu Y, Zhang Z, Chen M, Zhang D, Tian C, et al. The Antibacterial Activity and Mechanism of Action of Luteolin Against Trueperella pyogenes . Infect Drug Resist [Internet]. 2020 Jun 10 [cited 2025 Nov 17];13:1697–711. Available from:.

Habel JR, Nguyen AT, Rowntree LC, Szeto C, Mifsud NA, Clemens EB, et al. HLA-A*11:01-restricted CD8+ T cell immunity against influenza A and influenza B viruses. *PLoS Pathog.* 2022 Mar 1;18(3):e1010337.

Horemans S, Pitoulias M, Holland A, Pateau E, Lechaplais C, Ekaterina D, et al. Pyruvate kinase, a metabolic sensor powering glycolysis, drives the metabolic control of DNA replication. *BMC Biol.* 2022 Apr 13;20(1):1–25.

How SS, Nathan S, Lam SD, Chieng S. ATP-binding cassette (ABC) transporters: structures and roles in bacterial pathogenesis. J Zhejiang Univ Sci B [Internet]. 2024 Mar 1 [cited 2025 Dec 2];26(1):58. Available from: https://pmc.ncbi.nlm.nih.gov/articles/PMC11735909/

Jajere SM. A review of *Salmonella enterica* with particular focus on the pathogenicity and virulence factors, host specificity and antimicrobial resistance including multidrug resistance. Vet World. 2019;12(4):504.

Jensen KK, Andreatta M, Marcatili P, Buus S, Greenbaum JA, Yan Z, et al. Improved methods for predicting peptide binding affinity to MHC class II molecules. *Immunology.* 2018 Jul 1;154(3):394–406.

Jespersen CM, Peters B, Nielsen M, and Marcatili P. BepiPred-2.0: improving sequence-based B-cell epitope prediction using conformational epitopes. Nucleic Acids Res [Internet]. 2017 Jul 3 [cited 2025 May 22];45(W1):W24–9. Available from: https://dx.doi.org/10.1093/nar/gkx346

Kashyap D, Khan A, and Lahare B. Pathogenic Protein Identification and Localization Prediction in Pseudomonas fuscovaginae: A Study on Sheath Brown Rot in Rice. 2020;XXIX, No 1:150–60.

Kovács D, Pézsa PN, Móritz VA, Jerzsele Á, and Farkas O. Effects of Luteolin in an In Vitro Model of Porcine Intestinal Infections. Animals. 2024 Jul 1;14(13).

Liu X, Dong W, Zhang Y, Tian Y, Xiao Y, Yang M, et al. In vitro and in vivo evaluation of antibacterial activity and mechanism of luteolin from Humulus scandens against *Escherichia coli* from chicken. Poult Sci. 2024 Nov 1;103(11).

Murray CJ, Ikuta KS, Sharara F, Swetschinski L, Robles Aguilar G, Gray A, et al. Global burden of bacterial antimicrobial resistance in 2019: a systematic analysis. The Lancet. 2022 Feb 12;399(10325):629–55.

Mohsen Y, Tarchichi N, Barakat R, Kawtharani I, Ghandour R, Ezzeddine Z, et al. The Different Types of Metallophores Produced by *Salmonella enterica*: A Review. Microbiology Research 2023, Vol 14, Pages 1457-1469 [Internet]. 2023 Sep 19 [cited 2025 Nov 13];14(3):1457–69. Available from: https://www.mdpi.com/2036-7481/14/3/99/htm

Naidoo N, and Zishiri TO. Presence, Pathogenicity, Antibiotic Resistance, and Virulence Factors of *Escherichia coli*: A Review. Bacteria 2025, Vol 4, Page 16 [Internet]. 2025 Mar 11 [cited 2025 May 20];4(1):16. Available from: https://www.mdpi.com/2674-1334/4/1/16/htm

Pakbin B, Brück WM, Rossen JWA. Virulence factors of enteric pathogenic *Escherichia coli*: A review. Vol. 22, International Journal of Molecular Sciences. MDPI; 2021.

Potocnakova L, Bhide M, Pulzova LB. An Introduction to B-Cell Epitope Mapping and In Silico Epitope Prediction. J Immunol Res [Internet]. 2016 Jan 1 [cited 2025 Nov 7];2016(1):6760830. Available from: /doi/pdf/10.1155/2016/6760830.

Reynisson B, Alvarez B, Paul S, Peters B, Nielsen M. NetMHCpan-4.1 and NetMHCIIpan-4.0: improved predictions of MHC antigen presentation by concurrent motif deconvolution and integration of MS MHC eluted ligand data. Nucleic Acids Res [Internet]. 2020 Jul 2 [cited 2025 Nov 8];48(W1):W449–54. Available from: https://dx.doi.org/10.1093/nar/gkaa379.

Saha S, dan Raghava GPS. VICMpred: An SVM-based Method for the Prediction of Functional Proteins of Gram-negative Bacteria Using Amino Acid Patterns and Composition. Genomics Proteomics Bioinformatics [Internet]. 2006 Jan 1 [cited 2025 May 22];4(1):42–7. Available from: https://www.sciencedirect.com/science/article/pii/S1672022906600156

Singh M, Penmatsa A, Nandi D. Functional Characterization of Salmonella Typhimurium Encoded YciF, a Domain of Unknown Function (DUF892) Family Protein, and Its Role in Protection during Bile and Oxidative Stress. J Bacteriol [Internet]. 2023 Jul 1 [cited 2025 Nov 13];205(7):e00059-23. Available from: https://pmc.ncbi.nlm.nih.gov/articles/PMC10367587/.

Szklarczyk D, Santos A, Von Mering C, Jensen JL, Bork P, and Kuhn M. STITCH 5: augmenting protein–chemical interaction networks with tissue and affinity data. Nucleic Acids Res [Internet]. 2016 Jan 4 [cited 2025 May 22];44(D1):D380–4. Available from: https://dx.doi.org/10.1093/nar/gkv1277

Tadros DM, Racle J, Gfeller D. Predicting MHC-I ligands across alleles and species: how far can we go? Genome Medicine 2025 17:1 [Internet]. 2025 Mar 20 [cited 2025 Nov 8];17(1):1–13. Available from: https://genomemedicine.biomedcentral.com/articles/10.1186/s13073-025-01450-8.

Uppalapati SR, Vazquez-Torres A. Manganese Utilization in Salmonella Pathogenesis: Beyond the Canonical Antioxidant Response. Front Cell Dev Biol [Internet]. 2022 Jul 12 [cited 2025 Dec 1];10:924925. Available from: https://pmc.ncbi.nlm.nih.gov/articles/PMC9315381/.

Venus Lau WY, Hoad GR, Jin V, Winsor GL, Madyan A, Gray KL, et al. PSORTdb 4.0: expanded and redesigned bacterial and archaeal protein subcellular localization database incorporating new secondary localizations. Nucleic Acids Res [Internet]. 2021 Jan 8 [cited 2025 Nov 8];49(D1):D803–8. Available from: https://dx.doi.org/10.1093/nar/gkaa1095.

Wang J, Xiong K, Pan Q, He W, Cong Y. Application of TonB-Dependent Transporters in Vaccine Development of Gram-Negative Bacteria. Front Cell Infect Microbiol [Internet]. 2021 Jan 27 [cited 2025 Nov 7];10:589115. Available from: https://pmc.ncbi.nlm.nih.gov/articles/PMC7873555/

Wasfi R, Hamed SM, Amer MA, Fahmy LI. *Proteus mirabilis* Biofilm: Development and Therapeutic Strategies. Front Cell Infect Microbiol [Internet]. 2020 Aug 14 [cited 2025 Nov 19];10:414. Available from: https://pmc.ncbi.nlm.nih.gov/articles/PMC7456845/.